

Difference between bending and stretching moduli of single-walled carbon nanotubes that are modeled as an elastic tube

Christopher M. DiBiasio, Michael A. Cullinan, and Martin L. Culpepper

Citation: *Appl. Phys. Lett.* **90**, 203116 (2007); doi: 10.1063/1.2741144

View online: <http://dx.doi.org/10.1063/1.2741144>

View Table of Contents: <http://apl.aip.org/resource/1/APPLAB/v90/i20>

Published by the [American Institute of Physics](http://www.aip.org).

Related Articles

Phase coexistence evolution of nano BaTiO₃ as function of particle sizes and temperatures
J. Appl. Phys. **112**, 064110 (2012)

Nanoscale frictional characteristics of graphene nanoribbons
Appl. Phys. Lett. **101**, 123104 (2012)

Effect of stacking fault and temperature on deformation behaviors of nanocrystalline Mg
J. Appl. Phys. **112**, 054322 (2012)

Size effects on the impact response of copper nanobeams
J. Appl. Phys. **111**, 113512 (2012)

Symmetry of atomistic structure for armchair-edge graphene nanoribbons under uniaxial strain
Appl. Phys. Lett. **100**, 153112 (2012)

Additional information on *Appl. Phys. Lett.*

Journal Homepage: <http://apl.aip.org/>

Journal Information: http://apl.aip.org/about/about_the_journal

Top downloads: http://apl.aip.org/features/most_downloaded

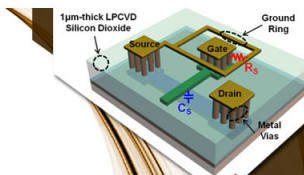
Information for Authors: <http://apl.aip.org/authors>

ADVERTISEMENT



**EXPLORE WHAT'S
NEW IN APL**

SUBMIT YOUR PAPER NOW!



SURFACES AND INTERFACES

Focusing on physical, chemical, biological, structural, optical, magnetic and electrical properties of surfaces and interfaces, and more...



ENERGY CONVERSION AND STORAGE

Focusing on all aspects of static and dynamic energy conversion, energy storage, photovoltaics, solar fuels, batteries, capacitors, thermoelectrics, and more...

Difference between bending and stretching moduli of single-walled carbon nanotubes that are modeled as an elastic tube

Christopher M. DiBiasio, Michael A. Cullinan, and Martin L. Culpepper^{a)}

Department of Mechanical Engineering, Massachusetts Institute of Technology, Cambridge, Massachusetts 02139

(Received 27 February 2007; accepted 26 April 2007; published online 18 May 2007)

The authors show that an elastic tube model of a (5,5) carbon nanotube predicts stretching and bending moduli that differ by 19%. This is due to (1) differing energy storage mechanisms in each mode and (2) the inability of the tube model to capture these effects. Conventional tube models assume a common energy storage mechanism in stretching and bending. They show that energy is stored primarily through bond stretching/rotation and bond torsion/van der Waals interactions in stretching and bending, respectively. This knowledge underscores the need to use different moduli to predict stretching, bending, and combined bending and stretching when using the tube model.

© 2007 American Institute of Physics. [DOI: 10.1063/1.2741144]

Carbon nanotubes (CNTs) are attractive for use in compliant nanomechanical devices due to their strength-strain characteristics.^{1,2} These characteristics have been exploited in work on CNT-based memory,³ flexure bearings,⁴ and resonators.⁵ Solid mechanics models are often used to model the behavior of these devices or to interpret measured device behaviors. These models require a material-specific metric that links load and deformation via geometry parameters. The elastic tube model, which is commonly applied to CNTs, relies upon a single value of an isotropic elastic modulus E to model axial stretching (AS) and lateral bending (LB) deformations. This approach is only accurate if the energy storage mechanisms in both modes are the same; however, there is no physical basis for making this assumption when modeling CNTs. We show that there are differences in the ways that a (5,5) CNT stores energy in LB and AS. The implications of these findings are that (1) modulus values determined from experiments/simulations with one mode of deformation (e.g., LB) should not be used to model or predict the other deformation mode (e.g., AS) and (2) CNTs that undergo combined AS and LB loading must be modeled with two moduli. For instance, the CNTs in Fig. 1 experience simultaneous AS and LB. This condition is experienced in CNT-based memory³ and resonators.⁵

The literature shows evidence that the LB and AS moduli differ. Commonly cited^{6–16} values for single-walled CNTs (SWCNTs) possess an average difference between moduli of 55%. These values correspond to an assumed tube wall thickness t (0.066–0.340 nm). As t changes, the modulus predicted by the tube model changes according to the equations that link tube behavior with tube thickness. This effect, known as Yakobson's paradox, compels us to use the membrane stiffness, $E \cdot t$,¹⁷ in order to mitigate thickness-related differences in modulus and to provide a more meaningful comparison between LB and AS moduli. With this metric, the average LB value is 12% larger than its AS counterpart. The average modulus value, and the membrane stiffness values, for LB exceed the AS values and this finding impelled the following work.

We used simulations to ascertain (a) the reasons why the moduli differ and (b) understand how the tube thickness affects the difference between the moduli. The latter is similar to Yakobson's paradox, but differs because we are contrasting moduli for different deformation modes.

In this work, tube stiffness values were obtained from a molecular model that consisted of a (5,5) CNT that contained 640 atoms. The tube's proximal end was grounded. In the AS simulations, the distal end of the tube was loaded with a force that was parallel to the CNT axis. A lateral force was applied to the distal end of the tube during the LB simulations. Atoms within the terminal cross section at the distal end were constrained such that the cross section remained circular. Elastomechanic characteristics were obtained via molecular mechanics simulations using the MM+force field and a Polak-Ribiere algorithm with a convergence criterion of 1 cal/mol Å. Van der Waals cutoffs were not used.

The LB stiffness, k_{bending} and AS stiffness, k_{axial} were used to calculate the corresponding membrane stiffness using the elastic tube model¹⁸ as embodied in Eqs. (1)–(4). Here L (7.64 nm) was the tube length, t (0.075 nm)¹⁹ was the wall thickness, and D was the tube diameter (0.68 nm).

$$E_{\text{axial}} = \frac{k_{\text{axial}}L}{A} \quad (1)$$

$$E_{\text{bending}} = \frac{k_{\text{bending}}L^3}{3I} \quad (2)$$

$$A = \frac{\pi}{4}[(D+t)^2 - (D-t)^2] \quad (3)$$

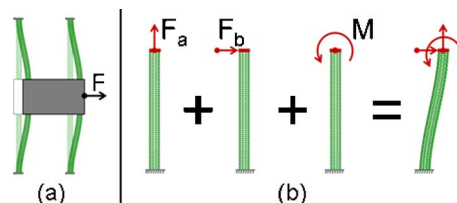


FIG. 1. (Color online) CNT-based shuttle that guides linear motion when actuated by force F (a) and combined loading on the shuttle's CNTs (b).

^{a)}Electronic mail: culpepper@mit.edu

TABLE I. Components of energy in a (5,5) CNT during AS and LB.

	AS (13.14 nN load)		LB (0.79 nN load)	
	ΔU (eV)	% of total ΔU	ΔU (eV)	% of total ΔU
Stretch	6.25	79.16	2.73	34.98
Bend	6.42	81.22	4.10	52.58
Torsion	-3.56	-45.13	0.37	4.70
van der Waals	-1.21	-15.25	0.60	7.75

$$I = \frac{\pi}{64} [(D+t)^4 - (D-t)^4]. \quad (4)$$

We obtained (1) an AS stiffness of 67.33 N/m which equates to $E \cdot t = 242$ N/m, and (2) a LB stiffness of 0.24 N/m which equates to $E \cdot t = 291$ N/m. The LB membrane stiffness is 19.3% higher than our AS membrane stiffness. There are two possible reasons for the difference. First the modes of energy storage in AS and LB could be different and this would lead to stiffness values that are not consistent with an assumption of equal moduli. Second, the tube model may not capture the difference between moduli and so this model may not be well suited as a modeling tool. The remainder of this letter examines both possibilities.

We found that the (5,5) SWCNT stored energy via different mechanisms during AS and LB. Our simulation results were examined to obtain information about the change in the amount of energy, ΔU , that is stored in the force field components. This data is listed in Table I. Inspection of the percent change columns reveals that the magnitude of the changes associated with each component are different in the AS and LB cases. This shows that energy is stored via different mechanisms in AS and LB, and therefore it is unwise to assume equal moduli for AS and LB.

Understanding the reasons for this behavior requires examination of the strain and geometry changes in the CNT lattice during loading and the corresponding changes in potentials. We will discuss AS and LB separately.

Under AS, van der Waals energy is decreased because the nonbonded atoms in the aromatic ring move further apart and closer to their equilibrium distance. In addition, the distance between the carbon atoms in each unit cell increases, which in turn increases the distance between the p -orbitals that make up the delocalized π bonds. This is manifested as a reduction in the stored torsional energy.²⁰

In order to understand what transpires in the LB case, it is helpful to focus on the aromatic rings that are shown in

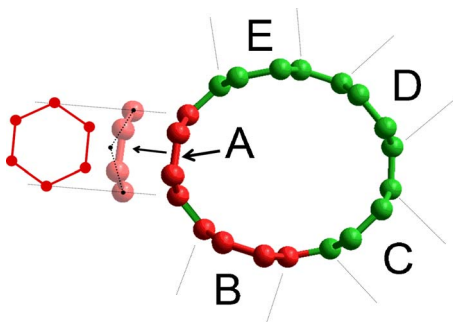


FIG. 2. (Color online) View of a (5,5) SWCNT unit cell in LB due under a 0.79 nN load.

TABLE II. Change in van der Waals energy during LB (0.79 nN load).

	Proximal (eV)	Middle (eV)	Distal (eV)
A	0.03	0.01	-0.01
B	0.18	0.06	0.01
C	0.13	0.05	0.01
D	-0.03	-0.03	0.00
E	-0.08	-0.05	-0.01

Fig. 2, and the data that is presented in Tables II and III. Table II shows that rings D and E generally experience a decrease in van der Waals potential because they undergo strain that brings the nonbonded atoms closer to their equilibrium distance. Rings B and C primarily experience compressive strain that drives the nonbonded atoms away from their equilibrium position. The asymmetry of the van der Waals potential function about the equilibrium position may be used to show that the van der Waals energy stored via compressive strain (rings B and C) is larger than the energy released through a tensile strain of equal magnitude (rings D and E). Ring A is located near the neutral axis of the tube and experiences little axial strain. Therefore, ring A does not contribute a significant amount to the van der Waals potential. Given the preceding, one would expect the van der Waals potential to increase and this is consistent with the data presented in Tables I and II.

We now discuss the torsion potential in the LB case. Changes in this potential are linked to changes in the p -orbital spacing. The change in spacing may be caused by (a) axial strain that would change the spacing of the p -orbitals in directions that are parallel to the axis of the tube or (b) a change in the local radius of curvature within the cross section of the tube. With respect to the former, rings D and E experience tensile strain (a decrease in potential) and rings B and C experience compressive strain (an increase in potential). With respect to the latter, at the sides of the tube (rings A, C, and D in Fig. 2) the radius of curvature decreases and causes the torsional energy to increase. This is due to the interaction between delocalized π bonds that resist the bending of the aromatic ring in out-of-plane directions.

These changes in potential are quantified in Table III. The table shows the change in torsional energy for aromatic rings within three unit cells. The cells are located at the proximal, middle, and distal portions of the tube. For each unit cell, the increase in torsional energy in rings A, B, and C are essentially offset by the decrease in torsional energy in rings D and E. As such, one would expect little change in the torsional energy and this is reflected in Table I as the torsional energy increase is 4.7% of the total increase in stored energy during LB.

TABLE III. Change in torsional energy during LB under a 0.79 nN load.

	Proximal (eV)	Middle (eV)	Distal (eV)
A	0.36	0.12	0.00
B	0.19	0.12	0.04
C	0.38	0.17	0.03
D	-0.01	-0.06	-0.03
E	-0.69	-0.32	-0.07

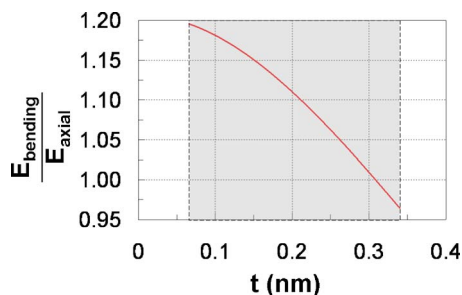


FIG. 3. (Color online) Change in ratio of LB and AS moduli as a function of thickness for a (5,5) SWCNT.

The small increase in the torsional and van der Waals potentials during LB contrasts with the large decrease in torsion and van der Waals potentials during AS. As such, energy is stored via different mechanisms in AS and LB. The force field components associated with the different mechanisms have different fundamental relationships between strain and energy storage. The elastic modulus may be used to link energy to the deformation of a part via geometric parameters of the deformed part. It therefore follows that different energy storage mechanisms mean that there must be different modulus values.

The preceding provides a basis for a difference to exist between the moduli. It is also important to understand the inherent limitations of the tube model, e.g., Eqs. (1)–(4), in relating the moduli during AS and LB. The difference in modulus values (1) is subject to the use of a consistent thickness when modeling AS and LB and (2) is a function of the assumed thickness. We calculated the ratio of LB to AS moduli using (a) the tube model described by Eqs. (1)–(4) and (b) the simulated stiffness values from our molecular models. The ratio-thickness relationship is plotted in Fig. 3.

It might be tempting to select a thickness that is large enough to make the tube model predict that the two moduli are equal, but this is problematic. In the (5,5) tube the thickness would exceed 90% of the radius and this would not be

a faithful representation of the CNT's structure.

In this letter, we show that it is not generally appropriate to use a single value of modulus when an elastic tube model is used to predict the AS and LB of a (5,5) CNT. We have shown that the difference in moduli is due to (1) differences in energy storage mechanisms and (2) inconsistencies caused by the use of the elastic tube model. Current efforts are focused on using these results to design CNT-based nanomechanical devices that rely on combined loading.

- ¹S. Iijima, *Nature (London)* **354**, 56 (1991).
- ²J. Lu and L. Zhang, *Comput. Mater. Sci.* **35**, 432 (2006).
- ³T. Ruckes, K. Kim, E. Joselevich, G. Y. Tseng, C. Cheung, and C. M. Lieber, *Science* **289**, 94 (2000).
- ⁴M. L. Culpepper, C. M. DiBiasio, R. M. Panas, S. Maglby, and L. H. Howell, *Appl. Phys. Lett.* **89**, 203111 (2006).
- ⁵B. Witkamp, M. Poot, and H. S. J. van der Zant, *Nano Lett.* **6**, 2904 (2006).
- ⁶C. Li and T. W. Chou, *Int. J. Solids Struct.* **40**, 2487 (2003).
- ⁷E. Hernandez, C. Goze, P. Bernier, and A. Rubio, *Phys. Rev. Lett.* **80**, 4502 (1998).
- ⁸A. L. Kalamkarov, A. V. Georgiades, S. K. Rokkam, V. P. Veedu, and M. N. Ghasemi-Nejhad, *Int. J. Solids Struct.* **43**, 6832 (2006).
- ⁹K. N. Kudin, G. E. Scuseria, and B. I. Yakobson, *Phys. Rev. B* **64**, 235406 (2001).
- ¹⁰J. P. Lu, *Phys. Rev. Lett.* **79**, 1297 (1997).
- ¹¹D. Sanchez-Portal, E. Artacho, J. M. Soler, A. Rubio, and P. Ordejon, *Phys. Rev. B* **59**, 12678 (1999).
- ¹²B. I. Yakobson, C. J. Brabec, and J. Bernholc, *Phys. Rev. Lett.* **76**, 2511 (1996).
- ¹³J. P. Salvetat, G. A. D. Briggs, J. M. Bonard, R. R. Bacsa, A. J. Kulik, and T. Stockli, *Phys. Rev. Lett.* **82**, 944 (1999).
- ¹⁴A. Krishnan, E. Dujardin, T. W. Ebbesen, P. N. Yianilos, and M. M. J. Treacy, *Phys. Rev. B* **58**, 14013 (1998).
- ¹⁵A. Sears and R. C. Batra, *Phys. Rev. B* **69**, 235406 (2004).
- ¹⁶X. Chen and G. Cao, *Nanotechnology* **17**, 1004 (2006).
- ¹⁷Y. Huang, J. Wu, and K. C. Hwang, *Phys. Rev. B* **74**, 245413 (2006).
- ¹⁸V. M. Harik, *Comput. Mater. Sci.* **24**, 328 (2002).
- ¹⁹A. Pantano, D. M. Parks, and M. C. Boyce, *J. Mech. Phys. Solids* **52**, 789 (2004).
- ²⁰A. R. Leach, *Molecular Modeling*, 2nd ed. (Prentice-Hall, Dorchester, UK, 2001), p. 176.